J. Math. Anal. Appl. 547 (2025) 129291

Contents lists available at ScienceDirect

Journal of Mathematical Analysis and Applications

journal homepage: www.elsevier.com/locate/jmaa

Regular Articles

Computing harmonic-measure distribution functions of some multiply connected unbounded planar domains

Arunmaran Mahenthiram

Department of Mathematics and Statistics, University of Jaffna, Jaffna 40000, Sri Lanka

A R T I C L E   I N F O

Article history:
Received 3 June 2024
Available online 21 January 2025
Submitted by D. Khavinson

Keywords:
Harmonic-measure distribution functions
Multiply connected domains
Prime functions
Conformal map

A B S T R A C T

A Brownian particle released from a point z_0 in a two-dimensional region Ω will move around randomly until it eventually hits the boundary of Ω. We are interested in the probability that it hits the boundary somewhere within distance r of the starting point z_0, for each value of r. Putting together these probabilities for all values of r gives a function $h(r)$ called the harmonic-measure distribution function or h-function of Ω with respect to z_0. This h-function encodes information about the shape of the boundary of Ω. In this paper, we compute the h-functions for some multiply connected planar regions whose boundary consists of collinear unequal slits or dissimilar discs. The key tool we use for computing these h-functions is a special function, called the *Schottky-Klein* prime function. Furthermore, we have validated our results by simulating the random motion of Brownian particles in the regions mentioned above.

© 2025 Elsevier Inc. All rights are reserved, including those for text and data mining, AI training, and similar technologies.

1. Introduction

This paper is focused on the computation of *harmonic-measure distribution functions* or *h-functions* of some new multiply connected planar domains whose connectivity is strictly greater than two. The domains on which we focus are unbounded and have the boundary as collinear line segments of different sizes or circles of different sizes. The computation of h-functions of higher connected domains is more complicated than the computation of h-functions of simply connected domains. For the computation of h-functions, we make extensive use of complex analysis techniques, especially conformal mappings and the conformal invariance of harmonic measure, as well as a deep connection between Brownian motion, harmonic measure and the Dirichlet problem. For multiply connected domains, we bring to bear the *Schottky–Klein prime function* which is simply called *prime function* denoted by $\omega(\zeta, \alpha)$. We also cross-check the validity of our theoretical h-functions we find by rederiving them via numerical simulation of Brownian motion.

E-mail address: arunmaran@univ.jfn.ac.lk.

https://doi.org/10.1016/j.jmaa.2025.129291
0022-247X/© 2025 Elsevier Inc. All rights are reserved, including those for text and data mining, AI training, and similar technologies.

The concept of h-function was introduced and first studied by Walden and Ward [24] after they were motivated via Ken Stephenson's questions on w-function posted in [3, Problem 6.116]. Stephenson's w-function is closely related to the h-function, but not exactly the same function. From Walden and Ward's initial paper [24] till now, the study of h-functions has been well-developed for simply connected domains by several authors. A summary of the progress (1996-2016) has been documented in the survey article [22]. Recently, new results regarding the h-functions of many simply connected regions have been obtained and are documented in [17], [18], [20], and [21]. Interestingly, some of these new h-functions show behaviour that was not previously known to occur.

Now, we describe the notion h-function for a domain Ω concerning a fixed point z_0 (basepoint) in the domain Ω. First, we describe the h-function $h_{\Omega,z_0}(r)$, for short $h(r)$, via the solution of the following Dirichlet problem:

$$\Delta u(z) = 0 \text{ if } z \in \Omega,$$
$$u(z) = \begin{cases} 1, & \text{if } z \in E_r; \\ 0, & \text{if } z \in \partial\Omega \backslash E_r, \end{cases}$$

where $E_r = \partial\Omega \cap \overline{B(z_0, r)}$ and $\partial\Omega$ denotes the boundary of the domain Ω. The h-function is given by the solution of the above Dirichlet problem at z_0. That is, $h(r) = u(z_0)$.

Alternatively, we can explain the h-function via the physical intuition of the Brownian motion. For a domain Ω in the complex plane $\mathbb{C}$, and a basepoint z_0 in Ω, the h-function is given by the probability that a particle released from the basepoint z_0 first exits the region within distance r of z_0. Since the h-function represents the probability, it will always be on the unit interval $[0, 1]$. Also, the h-function is an increasing and right-continuous. Moreover, this function is piecewise-defined for different ranges of r. These ranges are called *regimes of* r. For example, for the halfplane $\Omega = \{z \in \mathbb{C} : \operatorname{Im} z > 0\}$ with basepoint $z_0 = i$, the h-function is given by

$$h(r) = \begin{cases} 0, & \text{for } 0 < r < 1; \\ \dfrac{2}{\pi} \arctan\left\{ \dfrac{\sqrt{r^2 - d^2}}{d} \right\}, & \text{for } r \geq 1. \end{cases}$$

This h-function expression has two regimes of r, and the h-function $h(r)$ is zero for the first regime of $r : 0 < r < d = 1$; and is strictly positive for the second regime of $r : r \geq d = 1$.

For any domain Ω, the h-function will always be zero for the first regime of r, and need not be one for the last regime of r. However, for domains (bounded or unbounded) with bounded boundaries, the h-function $h(r)$ will take the value one for the last regime of r. When the boundary is unbounded, the function $h(r)$ will not attain the value one, but will approach the value one.

Now, we move on to the key tool that we use in the computation of h-functions of multiply connected planar domains. The key tool is the prime function which is an important transcendental function used to solve problems related to multiply connected domains. Crowdy's monograph [8] provides a full treatment of the prime function. Moreover, the prime function has been used in numerous applications involving multiply connected domains in the literature. For instance, see [4], [5], [6], [9], [16], [13] and [14]. Recently, the prime function has been used in the construction of a function called the squeezing function which is also related to multiply connected domains. See [23].

We now explain the computation of the prime function $\omega(\zeta, \alpha)$. Fast and accurate MATLAB codes, based around the novel methods presented in [9], are available for downloading. By using these MATLAB codes, we can compute the prime function for any finite connectivity. Other ways of computing the prime function are presented in [5] and [13], or one may directly code the prime function's infinite product representation (which may or may not always converge, and whose convergence properties are not fully understood).

Now, we turn to the different types of conformal maps that we use in this paper to compute the h-functions of multiply connected domains via prime functions. One such map is radial-slit conformal mapping in terms of the prime function. We use this conformal mapping to transform the bounded circular domain D_ζ onto our target domain whose boundaries are slits that emanate from the origin. These maps were expressed in terms of the prime functions by Crowdy and Marshall in [4]. Moreover, the so-called *Cayley-type maps* play an important role in the h-function computation via the prime functions. We note that Crowdy [8] is credited with coining the phrase Cayley-type maps when he discovered the crucial characteristics of a ratio of prime functions of a multiply-connected circular domain when the second arguments in the denominator and numerator are taken on the same boundary circle in D_ζ. This specific word was originally used in the monograph [8]. Prior tho this monograph, he called them *half-space slit mappings* in a previous review paper [7]. Please refer to Section 3.1 for a detailed explanation of Cayley-type maps.

The computation of h-functions of multiply connected domains is in its infancy; we know of a few papers in this direction. Aarao et al. [1] (unpublished) obtained the h-function for a plane with two deleted collinear line segments, using several numerical approximation methods. Recently, Green et al. [14] computed an explicit formula for the h-function for the above domain using the prime function. Specifically, the h-function was computed for the domain Ω_2 in the complex plane whose boundary consists of the intervals $[-1/2, -1/6]$ and $[1/6, 1/2]$ in the real line, with basepoint $z_0 = -3/2$. Also, this article [14] explains how to calculate the h-functions of higher connectivity symmetrical slit domains with even connectivity, again when the basepoint z_0 is fixed to the left of all boundary components. The boundary components are bounded line segments on the real axis, symmetrically placed about the imaginary axis. Recently, Mahenthiram [19] computed h-functions for several bounded and unbounded polygonal domains. Also, Green et al. [11] and [12] computed h-functions of several bounded and unbounded domains whose boundaries consist of finitely many parallel but non-collinear line segments, or concentric circular slits (arcs), with various locations of the basepoint.

In this paper, we explain the computation of h-function for higher connected asymmetrical slit domains whose boundary consists of the unequal length of collinear line segments when the basepoint is fixed strictly to the left for our choice of order of the line segments. Two key elements of this computational method using the prime function are as follows: Computing various canonical conformal mappings; and constructing specific harmonic functions. We also compute the h-function of the complement of several dissimilar discs when the basepoint is fixed strictly to the right of all discs. For all our examples in this paper, we use a numerical simulation technique to cross-check our h-function graphs obtained theoretically. We obtain close agreement between the graphs of theoretical h-functions and simulated h-functions. For a detailed explanation of the simulation, refer to Section 3.3.

In this paper, for the computation of the h-functions, we use the MATLAB package [10] which implements the general form of the prime function. Also, throughout this paper, the *capture circle* denotes the circle of radius r centred at the basepoint z_0.

This paper is organised as follows: In Section 2, we give some definitions and formulas that are related to the prime function. In Section 3, we explain the computational procedure of h-functions that we use throughout this paper. In Section 4, we explore the h-functions of asymmetrical slit domains when the basepoint is fixed strictly to left of all boundary components. In Section 5, we compute the h-functions of complement of unequal discs when the basepoint is fixed strictly to left of all boundary components. Finally, in Section 6, we give the conclusion for this paper.

2. Background

In this section, we present definitions and results used in this paper. This material all relates to the prime function $\omega(\zeta, \alpha)$ (see [8]) which is associated with the circular domain D_ζ which is formed by deleting subdiscs from the unit disc. Fig. 2.1 shows the Schematic of the quintuply bounded circular domain D_ζ.

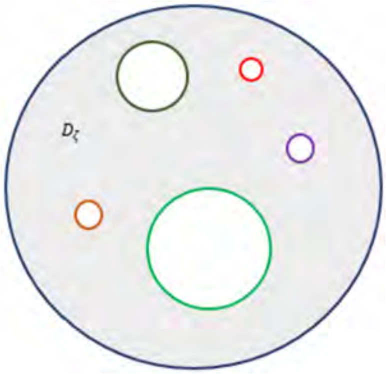

Fig. 2.1. Schematic of the bounded circular domain D_ζ in the sextuply connected setting.

First, we focus on the expressions of the prime function for the circular domains D_ζ with different connectivity. Let D_ζ be a bounded $(N+1)$-connected circular domain. According to Baker [2], the prime function is defined as

$$\omega(\zeta,\alpha) = (\zeta-\alpha)\prod_{\theta\in\Theta''}\frac{(\theta_i(\zeta)-\alpha)(\theta_i(\alpha)-\zeta)}{(\theta_i(\zeta)-\zeta)(\theta_i(\alpha)-\alpha)}, \tag{2.1}$$

where θ is a Möbius map that belongs to the group Θ'' which is a subgroup of the general Schottky group, and

$$\theta_j(\zeta) = \delta_j + \frac{q_j^2\zeta}{1-\bar{\delta}_j\zeta}, \ \ j = 1,\ldots,N.$$

Here δ_j, q_j are the centre and the radius respectively of the jth inner boundary circle C_j in the circular domain D_ζ. Moreover, for $\zeta,\tau\in C_j$,

$$\theta_j(\zeta) = 1/\bar{\zeta} \qquad \text{and} \qquad \overline{\theta_j}(1/\zeta) = \bar{\zeta}. \tag{2.2}$$

For the simply connected case, the circular domain D_ζ is the unit disc $\mathbb{D}$. In this case, the prime function takes the simple form

$$\omega(\zeta,\alpha) = \zeta-\alpha, \qquad \text{where } \ \zeta,\alpha\in\mathbb{D}.$$

Moreover, we use the general form $\omega(\zeta,\alpha)$ from equation (2.1) for multiply connected domains.

Note that for consistency, following [8] we use the same symbol D_ζ for the circular domain in the ζ-plane, whatever the connectivity. In particular, in this symbol D_ζ we make no reference to the parameters δ_j and q_j in the higher connectivity case, although these parameters determine the geometry of the particular circular domain D_ζ we are using.

The identities of the prime function $\omega(\zeta,\alpha)$ for the multiply connected domains D_ζ are as follows:

$$\bar{\omega}(1/\zeta,1/\alpha) = -\frac{1}{\zeta\alpha}\omega(\zeta,\alpha) \qquad \text{and} \qquad \omega(\zeta,\alpha) = -\omega(\alpha,\zeta), \tag{2.3}$$

where $\zeta,\alpha\in D_\zeta$. The derivation of these identities is discussed by Crowdy [8]. The prime function has the following important properties [15]:

$$\omega(\theta_j(\zeta),\alpha) = \gamma_j(\zeta,\alpha)\omega(\zeta,\alpha), \ \ j = 1,\ldots,N, \tag{2.4}$$

for the $(N+1)$ connectivity domain, where

$$\gamma_j(\zeta,\alpha) = \exp[-2\pi i\left(v_j(\zeta) - v_j(\alpha) + \frac{\tau_{jj}}{2}\right)]\sqrt{\theta_j'(\zeta)},$$

$v_j(\zeta)$ denotes the integrals of the first kind associated with D_ζ [8, pages 32-33], and τ_{jj} is a purely imaginary constant and θ_j' is the derivative of θ_j with respect to ζ. Moreover,

$$\frac{\omega(\theta_j(\zeta),\alpha_1)}{\omega(\theta_j(\zeta),\alpha_2)} = \exp[2\pi i(v_j(\alpha_1) - v_j(\alpha_2))]\frac{\omega(\zeta,\alpha_1)}{\omega(\zeta,\alpha_2)}, \tag{2.5}$$

where

$$v_j(\tau) = \bar{v}_j(1/\tau) = \overline{v_j(1/\bar{\tau})}. \tag{2.6}$$

For a detailed discussion of the above expressions, please refer to [8].

3. Procedure for computing h-functions using the prime function

In this section, we explain the process to calculate the h-functions of certain multiply connected domains by using the prime functions which are defined on the preimage domain, called bounded circular domain D_ζ. All domains have different formulas of prime functions based on the connectivity of the domain.

In Section 3.1, we discuss the Cayley-type conformal maps which play a major role in the computation of the h-functions for multiply connected domains via the prime functions. In Section 3.2, we describe the process that we follow to compute the h-functions throughout this paper. In section 3.3, we explain the simulation technique which is an alternative way to calculate the h-functions. We use this method to check our h-function graphs which are obtained theoretically.

3.1. Cayley-type conformal maps

In the computation of the h-functions for multiply connected domains, we use the appropriate Cayley-type maps in each case based on the location of the basepoint z_0 in the target domain Ω. By using this location of the basepoint z_0, we transform the boundary of the respective boundary circle in the bounded circular domain D_ζ to the real axis, and mapping the other circles in D_ζ to slits or lines. In all cases (for simply and multiply connected domains), we fix the argument of the respective Cayley-type function R such that $-\pi \le \arg R < \pi$.

For the simply connected case, the preimage bounded circular domain D_ζ is the interior of the unit disc $\mathbb{D}$. In this case, for any location of the basepoint z_0, our choice of the Cayley-type map always transforms the boundary of the unit disc $\mathbb{D}$ onto the real axis. Also, the interior of the unit disc is mapped onto the lower halfplane.

The classical Cayley map is

$$R(\zeta,\tau,\bar{\tau}) = -\frac{1}{\tau}\frac{\omega(\zeta,\tau)}{\omega(\zeta,\bar{\tau})} = -\frac{1}{\tau}\frac{(\zeta-\tau)}{(\zeta-\bar{\tau})}, \tag{3.1}$$

where $\tau = e^{i\phi}$ with $\operatorname{Im}\tau > 0$. This Cayley map $R(\zeta,\tau,\bar{\tau})$ will behave as explained above. Also, from the expression (3.1), this map is also the Möbius in the simply connected case.

In this paper, the computation of h-functions has been focused on the multiply connected domains when the basepoint z_0 is fixed strictly to the left or right of all boundary components of our target domain Ω. When the basepoint z_0 is fixed strictly to the left or to the right of all boundary components of the domain Ω, the whole portion of a boundary component will be enclosed by the capture circle, before starting to enclose the other boundary components in the domain Ω. Thus, we define an appropriate Cayley-type map that transforms the respective boundary circle (based on the boundary component partially covered by the capture circle in our target domain Ω) to the real axis, while the other boundary circles (in ∂D_ζ) are mapped to slits which emanate from the origin and lie in the lower halfplane.

3.2. How to compute h-functions using prime function

In this section, we describe the process that we follow in the computation of the h-functions throughout this paper. In Section 3.2.1, we describe the conformal map $f(\zeta)$ for the computation of the h-function. In Section 3.2.2, we explain the computation of the harmonic function $\operatorname{Im} W(\zeta)$.

We now explain how to implement the method of conformal mappings in this context. Note that, instead of the halfplane, we use the circular domain D_ζ formed by deleting appropriate subdiscs from the unit disc.

3.2.1. Computing the conformal map $f(\zeta)$ using prime function

To compute the h-function for our target domain Ω, we use appropriate conformal mappings to transplant a bounded circular domain D_ζ to our target domain Ω. The process of the h-function computation is as follows. First, we identify the preimage $\zeta_0 \in D_\zeta$ of the given basepoint $z_0 \in \Omega$. Second, we define an appropriate Cayley-type map based on the location of the basepoint z_0 in the target domain Ω. At last, we identify the argument of the Cayley-type map for all boundary circles in the circular domain D_ζ. We fix the argument based on our choice of the branch of the argument of the Cayley-type function.

3.2.2. Computing the harmonic function $\operatorname{Im} W(\zeta)$ using prime function

We will show how to define a potential function $W(\zeta)$ which consists of the logarithmic term of the Cayley-type map and some other terms based on the needed boundary values on the respective boundary circles in the circular domain D_ζ. Then, $\operatorname{Im}[W(\zeta)]$ at $\zeta = \zeta_0$ gives the h-function for our target domain Ω.

3.3. Numerical simulation

We cross-check the h-function formulations that we got from prime functions using numerical simulation of Brownian motion. Think of a domain Ω, where z_0 is the basepoint. Millions of Brownian particles are now released from z_0, and their exit positions, where they first encounter the boundary $\partial\Omega$, are tracked. The number $h(r)$ can be approximated given $r > 0$, by counting the fraction of Brownian particles that hit $\partial\Omega$ within distance r of z_0. This approximate value will generally be more accurate the more simulation runs that are performed.

We compute the simulated h-function of the provided domain Ω with regard to z_0 using this concept, which is implemented in MATLAB. The numerical simulation procedure that is outlined here is applied to every h-function that is documented in this paper. We achieved excellent agreement between the simulated and calculated h-functions in all cases.

We present the numerical simulation results in the form of figures in the following format. For ease of comparison, we display the graphs of the theoretically calculated h-function and the numerically simulated h-function together on the same axes on the right and left, respectively, of the equation. See for example Fig. 4.3.

4. *h*-functions for domains whose boundaries are line segments

The conformal map

$$f(\zeta) = A\frac{\omega(\zeta,\alpha)\omega(\zeta,1/\bar{\alpha})}{\omega(\zeta,\beta)\omega(\zeta,1/\bar{\beta})}, \tag{4.1}$$

$\alpha,\ \beta \in D_\zeta$, transforms a circular domain D_ζ onto a domain whose boundaries are the line segments which lie on rays, emanating from the origin, where A is constant. See [4].

In this section, we describe the h-functions of higher connectivity domains by using the radial-slit mapping which transforms the bounded circular domain D_ζ onto the domain with deleted line segments of the real axis. Note that, this section provides an extension of the work done by Green et al. for the computation of the h-function of multiply connected symmetrical slit domains in [14]. They first described the pathway of the computational process of the h-functions of even connected symmetrical-slit domains, and the image of the unit disc on the boundary ∂D_ζ is the left-most slit in the target slit domain, and the left-right symmetry between the slits was there. See Sections 5(a) and 5(b) in [14] for the detailed explanation. Also, since their domains are even connected and the boundary slits are of the same size and are symmetrically placed about the imaginary axis, the h-functions will be identical when the basepoint is fixed strictly to the left or right of all slits at the same distance from the imaginary axis.

In this section, we compute the h-function of a slit domain when the symmetry condition is removed and the slits are of different sizes, and the order of the slits is changed from [14]. We consider a triply connected asymmetrical slit domain whose boundary consists of the image of the unit disc as the right-most slit and the basepoint is fixed strictly to the left of the left-most slit in our slit domain. See Fig. 4.1. In this case, the formulas mentioned in Sections 5(a) and 5(b) of [14] are not applicable, as the order of the slits has been placed differently. Thus, we have to derive the expressions for the order of our slits. Moreover, when the symmetry condition is removed, the condition $\alpha = -\beta$ is no longer valid, and the number of unknowns will be increased compared to the symmetric case. We use the Newton iteration to identify all the unknowns by writing the equations based on the endpoints of the slits. In this way, our work is novel though we adapt the same technique that was used in [14]. We should derive the formulas as it solves our Dirichlet problem in the circular domain D_ζ.

In Section 4.1, we formulate a path to compute the h-function when the basepoint z_0 is fixed to the left of all boundary components in our target domain. In Section 4.2, we compute the h-function for a triply connected domain whose boundary components are three deleted unequal line segments (slits) of the real axis when the basepoint z_0 is situated strictly to the left of all boundary components. In addition, we check our h-function graph by adding a tiny additional slit on the real axis. We obtain a slight change in the h-function graph for the domain which consists of an additional tiny slit.

4.1. How to compute the h-function for complement of $N+\ 1$ equal or unequal line segments, with basepoint to left of them

Consider a bounded circular domain D_ζ which has inner boundaries as circles C_j, $j = 1, 2\ldots, N$ and the outer boundary as the unit circle C_0. We also fix all inner circles of D_ζ along the real axis. We respectively fix the line segments (slits) along the real axis in the target domain Ω_{N+1} where all are the images of the boundary circles $C_N,\ C_{N-1},\ \ldots,\ C_2,\ C_1,\ C_0$ from the basepoint z_0.

For multiply connected case, the equations (2.2), (2.3), (2.4), (2.5), and (2.6) are useful to obtain the argument of the Cayley-type maps in the higher connectivity domains.

Let τ, $\bar{\tau}$ be the preimage points of intersecting points on the boundary $\partial\Omega_{N+1}$ of the target domain Ω_{N+1} by the capture circle. Also, we note that the quantity $(v_j(\tau) - v_j(\bar{\tau}))$ is purely real since all inner circles C_j have real centres, $j = 1, 2, \ldots, N$.

(1) For τ, $\bar{\tau} \in C_0$, we consider

$$\widetilde{W}_0(\zeta,\tau,\bar{\tau}) = \frac{1}{\pi}\log S_0(\zeta,\tau,\bar{\tau}), \text{ where } S_0(\zeta,\tau,\bar{\tau}) = -\frac{1}{\tau}\frac{\omega(\zeta,\tau)}{\omega(\zeta,\bar{\tau})}.$$

The Cayley-type map S_0 transforms the outer circle C_0 in ∂D_ζ onto the real axis, and maps all N inner circles onto N slits which emanate from the origin and lie in the lower halfplane.

(I) When $\zeta \in C_0$, we have $\zeta\bar{\zeta} = 1$. Also,

$$\begin{aligned}
\overline{S_0(\zeta,\tau,\bar{\tau})} &= -\frac{1}{\bar{\tau}}\frac{\bar{\omega}(\bar{\zeta},\bar{\tau})}{\bar{\omega}(\bar{\zeta},\tau)} \\
&= -\tau\frac{\bar{\omega}(1/\zeta,1/\tau)}{\bar{\omega}(1/\zeta,1/\bar{\tau})} \\
&= -\frac{1}{\tau}\frac{\omega(\zeta,\tau)}{\omega(\zeta,\bar{\tau})} \\
&= S_0(\zeta,\tau,\bar{\tau}).
\end{aligned}$$

Thus, $\arg S_0 = k\pi$, where $k \in \mathbb{Z}$. By choosing $\arg S_0 \in [-\pi,\pi)$, we have $\arg S_0 = -\pi, 0$.

(II) For $\zeta \in C_j$, $j = 1,2,\ldots,N$,

$$S_0(\zeta,\tau,\bar{\tau}) = -\frac{1}{\tau}\frac{\omega(\theta_j(1/\bar{\zeta}),\tau)}{\omega(\theta_j(1/\bar{\zeta}),\bar{\tau})} = -\frac{1}{\tau}e^{2\pi i(v_j(\tau)-v_j(\bar{\tau}))}\frac{\omega(1/\bar{\zeta},\tau)}{\omega(1/\bar{\zeta},\bar{\tau})}.$$

Then,

$$\begin{aligned}
\overline{S_0(\zeta,\tau,\bar{\tau})} &= -\frac{1}{\bar{\tau}}e^{-2\pi i[\bar{v}_j(1/\tau)-\bar{v}_j(1/\bar{\tau})]}\frac{\bar{\omega}(1/\zeta,\bar{\tau})}{\bar{\omega}(1/\zeta,\tau)} \\
&= -\frac{1}{\bar{\tau}}e^{-2\pi i[v_j(\tau)-v_j(\bar{\tau})]}\frac{\bar{\tau}}{\tau}\frac{\omega(\zeta,\tau)}{\omega(\zeta,\bar{\tau})} \\
&= e^{-2\pi i[v_j(\tau)-v_j(\bar{\tau})]}S_0(\zeta,\tau,\bar{\tau}).
\end{aligned}$$

This gives,

$$\frac{S_0(\zeta,\tau,\bar{\tau})}{\overline{S_0(\zeta,\tau,\bar{\tau})}} = e^{2\pi i[v_j(\tau)-v_j(\bar{\tau})]}.$$

Thus,

$$\arg S_0(\zeta,\tau,\bar{\tau}) = \pi[v_j(\tau)-v_j(\bar{\tau})].$$

Hence,

$$\begin{aligned}
1 + \operatorname{Im}[\widetilde{W}_0(\zeta,\tau,\bar{\tau})] &= 1 + \frac{1}{\pi}\arg S_0(\zeta,\tau,\bar{\tau}) \\
&= \begin{cases} 1 + \frac{1}{\pi}\{-\pi,0\} = 0,1, & \text{for } \zeta \in C_0; \\ 1 + [v_j(\tau)-v_j(\bar{\tau})], & \text{for } \zeta \in C_j,\ j = 1,\ldots,N. \end{cases}
\end{aligned}$$

Now, we consider the potential function

$$W_0(\zeta,\tau,\bar{\tau}) = i + \widetilde{W}_0(\zeta,\tau,\bar{\tau}) - i\sum_{j=1}^{N}[v_j(\tau) - v_j(\bar{\tau})]\widetilde{\sigma}_j(\zeta),$$

where $\{v_j(\zeta)\}_{j=1}^{N}$ are the integrals of the first kind associated with the circular domain D_ζ and $\{\widetilde{\sigma}_j(\zeta)\}_{j=1}^{N}$ are the analytic extensions of the harmonic functions $\left\{\sigma_j(\zeta,\bar{\zeta})\right\}_{j=1}^{N}$ in D_ζ with

$$\sigma_j(\zeta,\bar{\zeta}) = \mathrm{Re}[\widetilde{\sigma}_j(\zeta)],\ j = 1,\dots,N,$$

where σ_j is the harmonic measure satisfying

$$\sigma_j = \begin{cases} 0, & \text{on } C_0; \\ 1, & \text{on } C_j; \\ 0, & \text{on } C_k,\ k \neq j,\ j \neq 0. \end{cases} \tag{4.2}$$

Now, the harmonic function

$$\mathrm{Im}[W_0(\zeta,\tau,\bar{\tau})] = 1 + \mathrm{Im}[\widetilde{W}_0(\zeta,\tau,\bar{\tau})] - \sum_{j=1}^{N}[v_j(\tau) - v_j(\bar{\tau})]\sigma_j(\zeta,\bar{\zeta}) \tag{4.3}$$

solves our Dirichlet problem in our circular domain D_ζ.

(2) For $\tau,\ \bar{\tau} \in C_k,\ k = 1,2,\dots,N$,

$$\widetilde{W}_k(\zeta,\tau,\bar{\tau}) = \frac{1}{\pi}\log S_k(\zeta,\tau,\bar{\tau}),\ \text{ where } S_k(\zeta,\tau,\bar{\tau}) = \frac{1}{(\tau-\delta_k)}\frac{\omega(\zeta,\tau)}{\omega(\zeta,\bar{\tau})},$$

$\delta_k \in \mathbb{R}$ is the centre of the circle C_k in ∂D_ζ. This Cayley-type map S_k transforms the boundary circle C_k onto the real axis and maps all the remaining boundary circles in ∂D_ζ onto slits which emanate from the origin and lie in the lower halfplane.

(I) When $\zeta \in C_0$, we have

$$\begin{aligned} S_k(\zeta,\tau,\bar{\tau}) &= \frac{1}{(\tau-\delta_k)}\frac{\omega(\zeta,\tau)}{\omega(\zeta,\bar{\tau})} \\ &= \frac{1}{(\tau-\delta_k)}\frac{\omega(\tau,\zeta)}{\omega(\bar{\tau},\zeta)} \\ &= \frac{1}{(\tau-\delta_k)}\frac{\omega(\theta_k(1/\bar{\tau}),\zeta)}{\omega(\theta_k(1/\tau),\zeta)} \\ &= \frac{1}{(\tau-\delta_k)}\frac{(\tau-\bar{\delta_k})}{(\bar{\tau}-\bar{\delta_k})}\frac{\bar{\tau}}{\tau}e^{2\pi i[v_k(1/\tau)-v_k(1/\bar{\tau})]}\frac{\omega(\zeta,1/\bar{\tau})}{\omega(\zeta,1/\tau)} \\ &= \frac{\bar{\tau}}{\tau}\frac{1}{(\bar{\tau}-\bar{\delta_k})}e^{2\pi i[v_k(1/\tau)-v_k(1/\bar{\tau})]}\frac{\omega(1/\bar{\zeta},1/\bar{\tau})}{\omega(1/\bar{\zeta},1/\tau)}. \end{aligned}$$

Then,

$$\begin{aligned}\overline{S_k(\zeta,\tau,\bar\tau)} &= \frac{\tau}{\bar\tau}\frac{1}{(\tau-\delta_k)}e^{-2\pi i[\bar v_k(1/\bar\tau)-\bar v_k(1/\tau)]}\frac{\bar\omega(1/\zeta,1/\tau)}{\bar\omega(1/\zeta,1/\bar\tau)}\\ &= \frac{\tau}{\bar\tau}\frac{1}{(\tau-\delta_k)}e^{-2\pi i[v_k(\bar\tau)-v_k(\tau)]}\frac{\bar\tau}{\tau}\frac{\omega(\zeta,\tau)}{\omega(\zeta,\bar\tau)}\\ &= e^{2\pi i[v_k(\tau)-v_k(\bar\tau)]}S_k(\zeta,\tau,\bar\tau).\end{aligned}$$

This gives,

$$\frac{S_k(\zeta,\tau,\bar\tau)}{\overline{S_k(\zeta,\tau,\bar\tau)}} = e^{-2\pi i[v_k(\tau)-v_k(\bar\tau)]}.$$

Thus,

$$\arg S_k(\zeta,\tau,\bar\tau) = -\pi[v_k(\tau)-v_k(\bar\tau)] + m_0\pi, \quad m_0\in\mathbb{Z}.$$

(II) For $\zeta\in C_k$,

$$\begin{aligned}S_k(\zeta,\tau,\bar\tau) &= \frac{1}{(\tau-\delta_k)}\frac{\omega(\theta_k(1/\bar\tau),\zeta)}{\omega(\theta_k(1/\tau),\zeta)}\\ &= \frac{1}{(\tau-\delta_k)}\frac{(\tau-\bar\delta_k)}{(\bar\tau-\bar\delta_k)}\frac{\bar\tau}{\tau}e^{2\pi i[v_k(1/\tau)-v_k(1/\bar\tau)]}\frac{\omega(\zeta,1/\bar\tau)}{\omega(\zeta,1/\tau)}\\ &= \frac{1}{(\bar\tau-\bar\delta_k)}\frac{\bar\tau}{\tau}e^{2\pi i[v_k(1/\tau)-v_k(1/\bar\tau)]}\frac{\omega(\theta_k(1/\bar\zeta),1/\bar\tau)}{\omega(\theta_k(1/\bar\zeta),1/\tau)}\\ &= \frac{\bar\tau}{\tau}\frac{1}{(\bar\tau-\bar\delta_k)}\frac{\omega(1/\bar\zeta,1/\bar\tau)}{\omega(1/\bar\zeta,1/\tau)}.\end{aligned}$$

Then,

$$\begin{aligned}\overline{S_k(\zeta,\tau,\bar\tau)} &= \frac{\tau}{\bar\tau}\frac{1}{(\tau-\delta_k)}\frac{\bar\omega(1/\zeta,1/\tau)}{\bar\omega(1/\zeta,1/\bar\tau)}\\ &= \frac{1}{(\tau-\delta_k)}\frac{\omega(\zeta,\tau)}{\omega(\zeta,\bar\tau)}\\ &= S_k(\zeta,\tau,\bar\tau).\end{aligned}$$

Thus, $\arg S_k = m_1\pi$, where $m_1\in\mathbb{Z}$. By choosing $\arg S_k\in[-\pi,\pi)$, we have $\arg S_k = -\pi, 0$.

(III) For $\zeta\in C_j$, $j\neq k$,

$$\begin{aligned}S_k(\zeta,\tau,\bar\tau) &= \frac{1}{(\tau-\delta_k)}\frac{\omega(\theta_k(1/\bar\tau),\zeta)}{\omega(\theta_k(1/\tau),\zeta)}\\ &= \frac{1}{(\tau-\delta_k)}\frac{(\tau-\bar\delta_k)}{(\bar\tau-\bar\delta_k)}\frac{\bar\tau}{\tau}e^{2\pi i[v_k(1/\tau)-v_k(1/\bar\tau)]}\frac{\omega(\zeta,1/\bar\tau)}{\omega(\zeta,1/\tau)}\\ &= \frac{1}{(\bar\tau-\bar\delta_k)}\frac{\bar\tau}{\tau}e^{2\pi i[v_k(1/\tau)-v_k(1/\bar\tau)]}\frac{\omega(\theta_j(1/\bar\zeta),1/\bar\tau)}{\omega(\theta_j(1/\bar\zeta),1/\tau)}\\ &= \frac{1}{(\bar\tau-\bar\delta_k)}\frac{\bar\tau}{\tau}e^{2\pi i[v_k(1/\tau)-v_k(1/\bar\tau)]}e^{-2\pi i[v_j(1/\tau)-v_j(1/\bar\tau)]}\frac{\omega(1/\bar\zeta,1/\bar\tau)}{\omega(1/\bar\zeta,1/\tau)}.\end{aligned}$$

Then,

$$\begin{aligned}
\overline{S_k(\zeta,\tau,\bar{\tau})} &= \frac{\tau}{\bar{\tau}}\frac{1}{(\tau-\delta_k)}e^{-2\pi i[\bar{v}_k(1/\bar{\tau})-\bar{v}_k(1/\tau)]}e^{2\pi i[\bar{v}_j(1/\bar{\tau})-\bar{v}_j(1/\tau)]}\frac{\bar{\omega}(1/\zeta,1/\tau)}{\bar{\omega}(1/\zeta,1/\bar{\tau})} \\
&= \frac{1}{(\tau-\delta_k)}e^{2\pi i[v_k(\tau)-v_k(\bar{\tau})]}e^{-2\pi i[v_j(\tau)-v_j(\bar{\tau})]}\frac{\omega(\zeta,\tau)}{\omega(\zeta,\bar{\tau})} \\
&= e^{2\pi i[v_k(\tau)-v_k(\bar{\tau})]}e^{-2\pi i[v_j(\tau)-v_j(\bar{\tau})]}S_k(\zeta,\tau,\bar{\tau}).
\end{aligned}$$

This gives

$$\frac{S_k(\zeta,\tau,\bar{\tau})}{\overline{S_k(\zeta,\tau,\bar{\tau})}} = e^{-2\pi i[v_k(\tau)-v_k(\bar{\tau})]}e^{2\pi i[v_j(\tau)-v_j(\bar{\tau})]}.$$

Hence,

$$\arg S_k(\zeta,\tau,\bar{\tau}) = -\pi[v_k(\tau)-v_k(\bar{\tau})] + \pi[v_j(\tau)-v_j(\bar{\tau})] + m\pi, \quad m\in\mathbb{Z}.$$

Thus,

$$\begin{aligned}
\operatorname{Im}[\widetilde{W}_k(\zeta,\tau,\bar{\tau})] &= \frac{1}{\pi}\arg S_k(\zeta,\tau,\bar{\tau}) \\
&= \begin{cases} \frac{1}{\pi}\{-\pi,0\} = -1,0, & \text{for } \zeta\in C_k; \\ -[v_k(\tau)-v_k(\bar{\tau})] + m_0, & \text{for } \zeta\in C_0; \\ -[v_k(\tau)-v_k(\bar{\tau})] + [v_j(\tau)-v_j(\bar{\tau})] + m, & \text{for } \zeta\in C_j,\ j\neq k,0. \end{cases}
\end{aligned}$$

Since we have incorrect boundary values along the circle C_k, we add 1 to obtain the correct boundary values 1,0. Also, we take $m_0 = -1$ and $m = -1, 0$. Hence,

$$1 + \operatorname{Im}[\widetilde{W}_k(\zeta,\tau,\bar{\tau})] = \begin{cases} 1 + \{-1,0\} = 0,1, & \text{for } \zeta\in C_k; \\ -[v_k(\tau)-v_k(\bar{\tau})], & \text{for } \zeta\in C_0; \\ -[v_k(\tau)-v_k(\bar{\tau})] + [v_j(\tau)-v_j(\bar{\tau})], & \text{for } \zeta\in C_j,\ j<k,\ j\neq 0; \\ 1 - [v_k(\tau)-v_k(\bar{\tau})] + [v_j(\tau)-v_j(\bar{\tau})], & \text{for } \zeta\in C_j,\ j>k,\ j\neq 0. \end{cases}$$

Now, we consider the potential function

$$W_k(\zeta,\tau,\bar{\tau}) = i + \widetilde{W}_k(\zeta,\tau,\bar{\tau}) + i[v_k(\tau)-v_k(\bar{\tau})](1-\widetilde{\sigma}_k(\zeta)) - i\sum_{j\neq 0,k}^{N}[v_j(\tau)-v_j(\bar{\tau})]\widetilde{\sigma}_j(\zeta)$$

Now, the harmonic function

$$\operatorname{Im}[W_k(\zeta,\tau,\bar{\tau})] = 1 + \operatorname{Im}[\widetilde{W}_k(\zeta,\tau,\bar{\tau})] + [v_k(\tau)-v_k(\bar{\tau})](1-\sigma_k(\zeta,\bar{\zeta})) - \sum_{j\neq 0,k}^{N}[v_j(\tau)-v_j(\bar{\tau})]\sigma_j(\zeta,\bar{\zeta}) \tag{4.4}$$

solves our Dirichlet problem in our circular domain D_ζ, and σ_j is defined above in the expression (4.2).

4.2. Complement of three unequal line segments, with basepoint to left of them

Consider the triply connected domain Ω_3 which is the complement of three unequal line segments of the real axis. We pick $\Omega_3 = \mathbb{C}\backslash([-0.4,-0.1]\cup[0.1,0.2]\cup[0.4,1])$ and fix the basepoint $z_0 = -1$ which

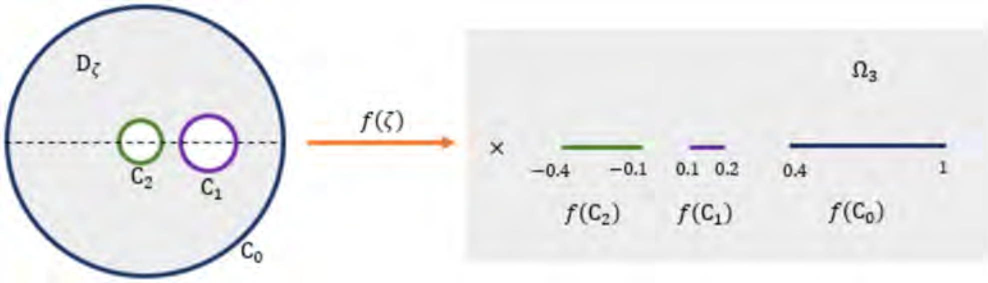

Fig. 4.1. Diagram of conformal map from triply connected bounded circular domain D_ζ to domain Ω_3.

is left of all line segments. Since our target domain Ω_3 is triply connected, our preimage domain D_ζ is a triply connected bounded circular domain which has three circles C_0, C_1 and C_2 as its boundary, where the circle C_2 is centred at the origin with radius q_2 and the circle C_1 is centred at δ_1 with radius q_1. The conformal map

$$f(\zeta) = A\frac{\omega(\zeta,\alpha)\omega(\zeta,1/\bar{\alpha})}{\omega(\zeta,\beta)\omega(\zeta,1/\bar{\beta})} \tag{4.5}$$

transforms the above D_ζ to the domain Ω_3. Since we fix the line segments along the real axis, we have the parameters $\alpha, \beta \in \mathbb{R}$ and these parameters lie in the preimage domain D_ζ. Thus, the conformal mapping formula (4.5) becomes

$$f(\zeta) = A\frac{\omega(\zeta,\alpha)\omega(\zeta,1/\alpha)}{\omega(\zeta,\beta)\omega(\zeta,1/\beta)}.$$

Also, in the domain Ω_3, the left-most, middle and right-most line segments are the preimages of boundary circles C_2, C_1 and C_0 respectively. See Fig. 4.1.

Also, we fix $f(-1) = 1$, $f(1) = 0.4$, $f(\delta_1 + q_1) = 0.2$, $f(\delta_1 - q_1) = 0.1$, $f(q_2) = -0.1$ and $f(-q_2) = -0.4$. By using $f(-1) = 1$, we express the constant A as follows:

$$A = \frac{\omega(-1,\beta)\omega(-1,1/\beta)}{\omega(-1,\alpha)\omega(-1,1/\alpha)}.$$

The preimages of the endpoints of each slit in the circular domain D_ζ are $-q_2$, q_2, $\delta_1 - q_1$, $\delta_1 + q_1$, 1 and -1. By using the multi-variable Newton's iteration, we find the unknowns δ_1, q_1, q_2, α and β as follows:

$$\begin{pmatrix}\delta_1\\ q_1\\ q_2\\ \alpha\\ \beta\end{pmatrix} \approx \begin{pmatrix}0.13711\\ 0.01783\\ 0.01454\\ 0.05861\\ -0.16693\end{pmatrix}.$$

Since $z_0 = -1 \in \Omega_3$, we use single-variable Newton's iteration to identify the preimage ζ_0 of the basepoint z_0. We identify $\zeta_0 \approx -0.07735\,(\in D_\zeta)$.

By using the MATLAB package of the prime function for the domains with higher connectivity (see [10]), we obtain the integrals of the first kind associated with this triply connected circular domain D_ζ as shown in Table 4.1.

Next, we turn to calculating the scalars c_{jk} for $j,k = 1,2$, we define

$$S_j(\zeta) = \sum_{k=1}^{2} c_{jk} v_k(\zeta)\ ;\ j = 1,2. \tag{4.6}$$

Table 4.1
Values for integrals of first kind associated with our triply connected bounded circular domain D_ζ.

$\mathrm{Im}[v_j(\zeta)]$	$\zeta \in C_1$	$\zeta \in C_2$
$j = 1$	0.63616	0.31621
$j = 2$	0.31621	0.67060

From (4.6), we write the following equations.

$$\mathrm{Im}[S_1(\zeta)] = \sigma_1(\zeta) = c_{11}\,\mathrm{Im}[v_1(\zeta)] + c_{12}\,\mathrm{Im}[v_2(\zeta)] \tag{4.7}$$

$$\mathrm{Im}[S_2(\zeta)] = \sigma_2(\zeta) = c_{21}\,\mathrm{Im}[v_1(\zeta)] + c_{22}\,\mathrm{Im}[v_2(\zeta)] \tag{4.8}$$

From (4.2) and (4.7), we have

$$\left.\begin{aligned} 1 &= c_{11}\,\mathrm{Im}[v_1(\zeta_1)] + c_{12}\,\mathrm{Im}[v_2(\zeta_1)] \quad \text{for} \quad \zeta_1 \in C_1 \\ 0 &= c_{11}\,\mathrm{Im}[v_1(\zeta_2)] + c_{12}\,\mathrm{Im}[v_2(\zeta_2)] \quad \text{for} \quad \zeta_2 \in C_2 \end{aligned}\right\}$$

Now, we express this as a matrix representation.

$$\begin{pmatrix} \mathrm{Im}[v_1(\zeta_1)] & \mathrm{Im}[v_2(\zeta_1)] \\ \mathrm{Im}[v_1(\zeta_2)] & \mathrm{Im}[v_2(\zeta_2)] \end{pmatrix} \begin{pmatrix} c_{11} \\ c_{12} \end{pmatrix} = \begin{pmatrix} 1 \\ 0 \end{pmatrix} \tag{4.9}$$

By substituting the values from Table 4.1 in (4.9), we obtain

$$c_{11} \approx 2.05315 \quad \text{and} \quad c_{12} \approx -0.96814.$$

Similarly, by using (4.2) and (4.8), we have

$$\begin{pmatrix} \mathrm{Im}[v_1(\zeta_1)] & \mathrm{Im}[v_2(\zeta_1)] \\ \mathrm{Im}[v_1(\zeta_2)] & \mathrm{Im}[v_2(\zeta_2)] \end{pmatrix} \begin{pmatrix} c_{21} \\ c_{22} \end{pmatrix} = \begin{pmatrix} 0 \\ 1 \end{pmatrix}, \tag{4.10}$$

where $\zeta_1 \in C_1$ and $\zeta_2 \in C_2$.
By substituting the values from Table 4.1 in (4.10), we obtain

$$c_{21} \approx -0.96814 \quad \text{and} \quad c_{22} \approx 1.94773.$$

To compute the harmonic measure of C_1, C_2 at the point ζ_0, we compute the integrals of the first kind associated with D_ζ. We have

$$\mathrm{Im}[v_j(\zeta_0)] \approx \begin{cases} 0.24977, & \text{for } j = 1; \\ 0.40559, & \text{for } j = 2. \end{cases}$$

Table 4.2 shows the computation of the harmonic measure at ζ_0.

Now, we move our focus in the discussion of the h-function of this triply connected slit domain Ω_3. We use the formulas which we derived in Section 4.1) for the $(N+1)$ connectivity domain whose only boundaries are the collinear line segments along the real axis.

Let z_r be the intersecting point on the boundary $\partial\Omega_3$ by the capture circle, where $f(\tau) = z_r = f(\bar{\tau})$ with $\mathrm{Im}\,\tau > 0$. See Fig. 4.2. This figure is drawn for $r \in [1.1, 1.2)$.

Table 4.2
Harmonic measure of C_1 and C_2 at ζ_0.

$\sigma_1(\zeta_0)$	$=$	$\mathrm{Im}[S_1(\zeta_0)]$	$\sigma_2(\zeta_0)$	$=$	$\mathrm{Im}[S_2(\zeta_0)]$
	$=$	$c_{11}\,\mathrm{Im}[v_1(\zeta_0)] + c_{12}\,\mathrm{Im}[v_2(\zeta_0)]$		$=$	$c_{21}\,\mathrm{Im}[v_1(\zeta_0)] + c_{22}\,\mathrm{Im}[v_2(\zeta_0)]$
	$=$	0.120148577920257		$=$	0.548159891522345
	$\approx$	0.120149.		$\approx$	0.548160.

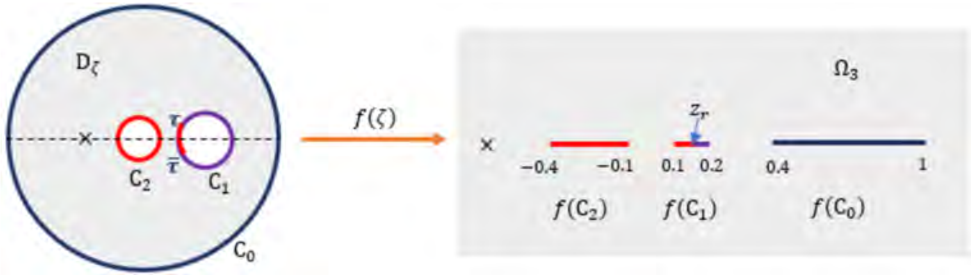

Fig. 4.2. Conformal map from triply connected bounded circular domain D_ζ to asymmetrical slit domain Ω_3 with basepoint $z_0 = -1$, for regime $1.1 \le r < 1.2$. The set E_r and its preimage are shown in red. (For interpretation of the colours in the figure(s), the reader is referred to the web version of this article.)

We know that the h-function $h(r)$ is zero for the regime $0 < r < 0.6$ as the capture circle does not intersect with any boundary component of Ω_3. Similarly, $h(r) = 1$ for the regime $r \ge 2$ as entire boundary $\partial\Omega_3$ is covered by the capture circle.

For the regime $0.6 \le r < 0.9$, the capture circle covers part of the left-most slit in $\partial\Omega_3$. In this case, $z_r \in [-0.4, -0.1)$ and $\tau, \bar{\tau}$ lie on the circle C_2 in ∂D_ζ, where $\tau = q_2 e^{i\phi}$, $\mathrm{Im}\,\tau > 0$ and ϕ varies from π to 0. By defining the function

$$W_2(\zeta,\tau,\bar{\tau}) = i + \frac{1}{\pi}\log\left[\frac{1}{(\tau-0)}\frac{\omega(\zeta,\tau)}{\omega(\zeta,\bar{\tau})}\right] + i[v_2(\tau)-v_2(\bar{\tau})][1-\widetilde{\sigma}_2(\zeta)] - i[v_1(\tau)-v_1(\bar{\tau})]\widetilde{\sigma}_1(\zeta),$$

we obtain $h(r) = \mathrm{Im}[W_2(\zeta_0,\tau,\bar{\tau})]$ for the regime $0.6 \le r < 0.9$.

For the regime $0.9 \le r < 1.1$, the capture circle covers the entire left-most slit (image of the circle C_2), but does not cover any part of the other two slits in $\partial\Omega_3$. In this case, $z_r \in [-0.1, 0.1)$. Also, $h(r) = \sigma_2(\zeta_0) \approx 0.54816$.

For the regime $1.1 \le r < 1.2$, the capture circle entirely covers the left-most slit in $\partial\Omega_3$ and part of the middle slit in $\partial\Omega_3$. In this case, $z_r \in [0.1, 0.2)$ and τ and $\bar{\tau}$ lie on the circle C_1 with $\tau = \delta_1 + q_1 e^{i\phi}$, $\mathrm{Im}\,\tau > 0$. Also, ϕ varies from π to 0. By defining the function

$$W_1(\zeta,\tau,\bar{\tau}) = i + \frac{1}{\pi}\log\left[\frac{1}{(\tau-\delta_1)}\frac{\omega(\zeta,\tau)}{\omega(\zeta,\bar{\tau})}\right] + i[v_1(\tau)-v_1(\bar{\tau})][1-\widetilde{\sigma}_1(\zeta)] - i[v_2(\tau)-v_2(\bar{\tau})]\widetilde{\sigma}_2(\zeta),$$

we obtain $h(r) = \mathrm{Im}[W_1(\zeta_0,\tau,\bar{\tau})]$ for the regime $1.1 \le r < 1.2$.

For the regime $1.2 \le r < 1.4$, the capture circle does not cover any part of the right-most slit in $\partial\Omega_3$, but entirely covers the other two slits in $\partial\Omega_3$. In this case, $z_r \in [0.2, 0.4)$. Also, $h(r) = \sigma_2(\zeta_0) + \sigma_1(\zeta_0) \approx 0.66831$.

For the regime $1.4 \le r < 2$, the capture circle covers part of the right-most slit in $\partial\Omega_3$, and also entirely covers the other two slits in $\partial\Omega_3$. In this case, $z_r \in [0.4, 1)$ and τ and $\bar{\tau}$ lie on the circle C_0 with $\tau = e^{i\phi}$, $\mathrm{Im}\,\tau > 0$. Also, ϕ varies from 0 to π. By defining the function

$$W_0(\zeta,\tau,\bar{\tau}) = i + \frac{1}{\pi}\log\left[-\frac{1}{\tau}\frac{\omega(\zeta,\tau)}{\omega(\zeta,\bar{\tau})}\right] - i\sum_{j=1}^{2}[v_j(\tau)-v_j(\bar{\tau})]\widetilde{\sigma}_j(\zeta),$$

we obtain $h(r) = \mathrm{Im}[W_0(\zeta_0,\tau,\bar{\tau})]$ for the regime $1.4 \le r < 2$.

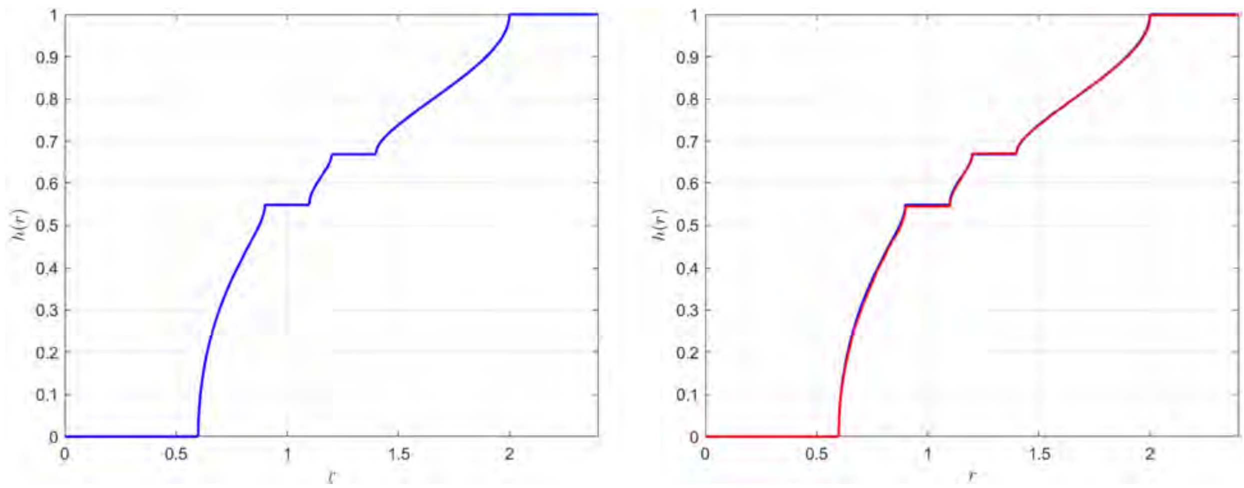

Fig. 4.3. Calculated h-function (left), and combination (right) of calculated (blue) and simulated (red) h-function for domain $\Omega_3 = \mathbb{C}\backslash([-0.4, -0.1] \cup [0.1, 0.2] \cup [0.4, 1])$ with basepoint $z_0 = -1$.

The h-function for the domain Ω_3 with basepoint $z_0 = -1$ is given by

$$h(r) = \begin{cases} 0, & \text{if } 0 < r < 0.6; \\ \mathrm{Im}[W_2(\zeta_0, \tau, \bar{\tau})], & \text{if } 0.6 \leq r < 0.9,\ |\tau| = q_2; \\ \sigma_2(\zeta_0), & \text{if } 0.9 \leq r < 1.1; \\ \mathrm{Im}[W_1(\zeta_0, \tau, \bar{\tau})], & \text{if } 1.1 \leq r < 1.2,\ |\tau - \delta_1| = q_1; \\ \sigma_2(\zeta_0) + \sigma_1(\zeta_0), & \text{if } 1.2 \leq r < 1.4; \\ \mathrm{Im}[W_0(\zeta_0, \tau, \bar{\tau})], & \text{if } 1.4 \leq r < 2,\ |\tau| = 1; \\ 1, & \text{if } r \geq 2, \end{cases} \tag{4.11}$$

where, $r = |f(\tau) - z_0|$.

Fig. 4.3 expresses the calculated (blue) and simulated (red) h-function graphs for the domain Ω_3 with basepoint $z_0 = -1$.

We now check our h-function graph shown in Fig. 4.3 by adding a tiny slit in addition to the three slits mentioned above. We add the tiny slit $[1, 015, 1.05]$ along the real axis. Now, our domain becomes quadruply connected which is $\Omega_4 = \mathbb{C}\backslash([-0.4, -0.1] \cup [0.1, 0.2] \cup [0.4, 1] \cup [1.015, 1.05])$. See Fig. 4.4. Also, the basepoint is still $z_0 = -1$. We do the similar calculations as we did in the triply connected case. First, we fix the slits in the same order as we considered in Ω_3. The only difference is the length of the new tiny slit, its position and the position of the preimage circles of all slits. Since the domain is quadruply connected, we consider a quadruply connected bounded circular domain D_ζ which has four circles C_0, C_1, C_2 and C_3 as its boundary, where the circle C_3 is centred at the origin with radius q_3, the circles C_2, C_1 have centres δ_2, δ_1 with radius q_2, q_1 respectively. As usual, C_0 is the unit circle. The conformal map

$$f(\zeta) = A\frac{\omega(\zeta, \alpha)\omega(\zeta, 1/\alpha)}{\omega(\zeta, \beta)\omega(\zeta, 1/\beta)}$$

transforms the new preimage domain D_ζ onto the quadruply connected slit domain Ω_4.

To find the seven unknowns in the preimage domain D_ζ, we fix $f(1) = 1.015$, $f(\delta_1 + q_1) = 1$, $f(\delta_1 - q_1) = 0.4$, $f(\delta_2 + q_2) = 0.2$, $f(\delta_2 - q_2) = 0.1$, $f(q_3) = -0.1$, $f(-q_3) = -0.4$. By using $f(-1) = 1.05$, we find the constant

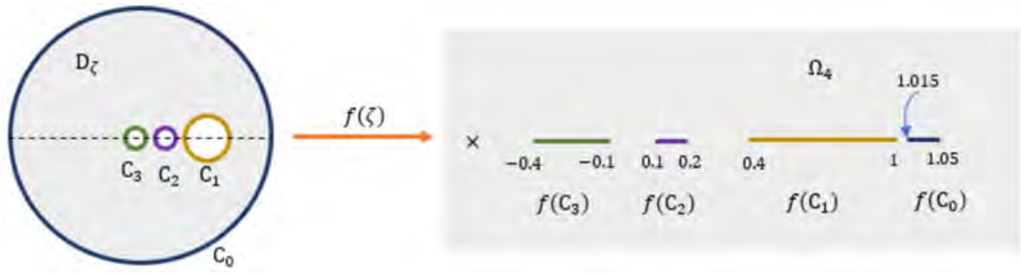

Fig. 4.4. Conformal transformation from quadruply connected bounded circular domain D_ζ to domain Ω_4.

Table 4.3
Values for integrals of first kind associated with our quadruply connected bounded circular domain D_ζ.

$\mathrm{Im}[v_j(\zeta)]$	$\zeta \in C_1$	$\zeta \in C_2$	$\zeta \in C_3$
$j = 1$	0.42025	0.38339	0.37187
$j = 2$	0.38339	0.98239	0.65074
$j = 3$	0.37187	0.65074	0.99347

Table 4.4
Values for scalars c_{jk}, $j, k = 1, 2, 3$ associated with our quadruply connected bounded circular domain D_ζ.

c_{jk}	$k = 1$	$k = 2$	$k = 3$
$j = 1$	4.06659	−1.02231	−0.85255
$j = 2$	−1.02231	2.05509	−0.96345
$j = 3$	−0.85255	−0.96345	1.95677

$$A = \frac{\omega(-1,\beta)\omega(-1,1/\beta)}{\omega(-1,\alpha)\omega(-1,1/\alpha)}.$$

By using multi-variable Newton's method, we identify the seven unknowns as follows:

$$\begin{pmatrix} \delta_1 \\ \delta_2 \\ q_1 \\ q_2 \\ q_3 \\ \alpha \\ \beta \end{pmatrix} \approx \begin{pmatrix} 0.09629 \\ 0.00700 \\ 0.07065 \\ 0.00077 \\ 0.00088 \\ 0.00331 \\ -0.01311 \end{pmatrix}.$$

Since the basepoint $z_0 = -1$, we find the preimage $\zeta_0 \approx -0.00523$ by using single-variable Newton's method.

Again, we use the formulas that we obtained for the general connectivity $N + 1$ by fixing $N = 3$. In this domain, we have three integrals of the first kind which are shown in Table 4.3.

Now, we obtain the scalars c_{jk}, $j, k = 1, 2, 3$, as shown in Table 4.4. The calculations are analogous to those in equations (4.6)–(4.10) for the triply connected domain; the 2×2 matrices there become 3×3 matrices here. We omit the details. Moreover,

$$\mathrm{Im}[v_j(\zeta_0)] \approx \begin{cases} 0.36375, & \text{for } j = 1; \\ 0.57610, & \text{for } j = 2; \\ 0.72023, & \text{for } j = 3. \end{cases} \tag{4.12}$$

Now, we consider the expression (4.6) with $j, k = 1, 2, 3$. Then, the imaginary part of this expression provides the harmonic measure of the circle C_j, $j = 1, 2, 3$ at the point ζ. To identify the harmonic measure at ζ_0, we

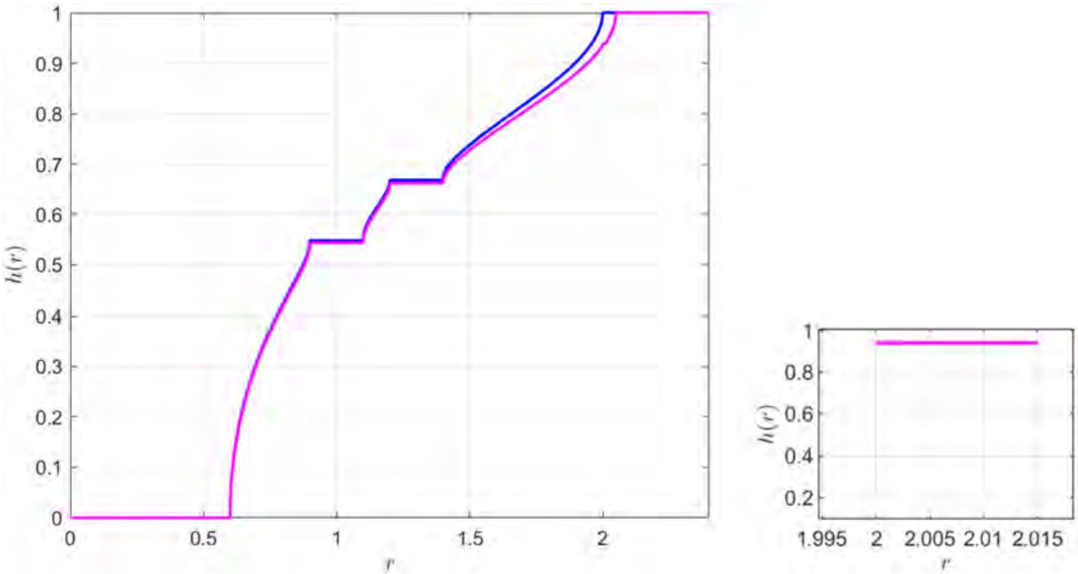

Fig. 4.5. Comparing h-functions for above two domains Ω_3 and Ω_4 with same basepoint z_0.

substitute the values of c_{jk} shown in Table 4.4 and in expression (4.12). Hence, we obtain $\sigma_1(\zeta_0) \approx 0.27625$, $\sigma_2(\zeta_0) \approx 0.11817$ and $\sigma_3(\zeta_0) \approx 0.54416$.

Moreover, the step heights h_1, h_2, h_3 are as follows:

$$h_1 = \sigma_3 \approx 0.54416;$$
$$h_2 = \sigma_3 + \sigma_2 \approx 0.66232;$$
$$h_3 = \sigma_3 + \sigma_2 + \sigma_1 \approx 0.93857.$$

Fig. 4.5 shows the comparison between the h-functions of the domains Ω_3 and Ω_4. In the left-hand image, the graph shown in magenta expresses the h-function for the domain Ω_4, while the graph shown in blue expresses the h-function for the domain Ω_3. Also, we see the step height for the smaller range of r from 2 to 2.015. The right-hand image of Fig. 4.5 shows the zoomed version of this step height h_3 for this smaller range of r.

5. *h*-functions for domains whose boundaries are circles

In this section, we explain the h-functions for the domain Ω_N whose boundary components are N-unequal-sized circles when the basepoint z_0 is fixed strictly to the right of all boundary circles. We consider the Möbius map which transforms an N-bounded circular domain D_ζ onto the domain Ω_N. In the domain Ω_N, we fix the circles in order as images of the boundary circles $C_0, \ldots, C_{N-1}$ from left to right respectively. When the basepoint z_0 is fixed to the right of all circles in the domain Ω_N, the formulas (4.3) and (4.4) hold. We first provide the discussion of the h-function of the quintuply connected domain Ω_5 when the basepoint z_0 is fixed strictly to the right of all five discs on the real axis in Ω_5.

Now, we consider a quintuply connected circular domain D_ζ whose boundaries are five circles C_0, C_1, C_2, C_3, C_4 and C_5, where the circle C_j is centred at δ_j with radius q_j, $j = 1, \ldots, 5$. The conformal map $f(\zeta) = 1/(2\zeta)$ provides the domain Ω_5 whose boundaries are five unequal circles.

In the domain Ω_5, we fix all the circles in the order $f(C_0)$, $f(C_1)$, ... , $f(C_4)$ from left to right, and has centres respectively at 0, 1.25, 2.4, 3.6, 4.75 with respective radius 0.5, 0.25, 0.6 0.4, 0.25. Now, we can find the position of the preimage circles in the preimage circular domain D_ζ via the conformal map f. Also,

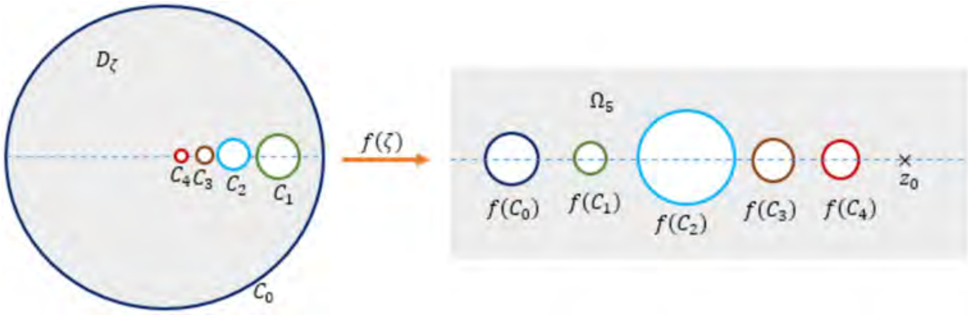

Fig. 5.1. Conformal map from quintuply connected bounded circular domain D_ζ to domain Ω_5 with discs of unequal size with basepoint $z_0 = 5.5$.

we fix the basepoint $z_0 = 5.5 \in \Omega_5$ which is right of all the circles in the target domain Ω_5. Then, its preimage ζ_0 can be found via $\zeta_0 = f^{-1}(z_0)$.

Fig. 5.1 shows the conformal transformation from the circular domain D_ζ to the quintuply connected domain Ω_5 with discs of unequal size.

As mentioned in the triply connected asymmetrical slit domain in Section 4.2, we can identify the integrals of the first kind $v_j(\zeta)$ and the scalars c_{jk}, $j,k = 1,2,3,4$ for our quintuply connected domain Ω_5. Also, we identified the harmonic measure at ζ_0 as follows:

$$\sigma_1(\zeta_0) \approx 0.02096,\ \sigma_2(\zeta_0) \approx 0.08566,\ \sigma_3(\zeta_0) \approx 0.11985 \text{ and } \sigma_4(\zeta_0) \approx 0.68948.$$

The formulas for the potential function $W_j(\zeta,\tau,\bar{\tau})$, $j = 0,1,2,3,4$ are the same as provided in the discussion of Section 4.1. Hence,

$$h(r) = \begin{cases} 0, & \text{if } 0 < r < 0.5; \\ \operatorname{Im}[W_4(\zeta_0,\tau,\bar{\tau})], & \text{if } 0.5 \le r < 1,\ |\tau - \delta_4| = q_4; \\ \sigma_4(\zeta_0) \approx 0.68948, & \text{if } 1 \le r < 1.5; \\ \operatorname{Im}[W_3(\zeta_0,\tau,\bar{\tau})], & \text{if } 1.5 \le r < 2.3,\ |\tau - \delta_3| = q_3; \\ \sigma_4(\zeta_0) + \sigma_3(\zeta_0) \approx 0.80933, & \text{if } 2.3 \le r < 2.5; \\ \operatorname{Im}[W_2(\zeta_0,\tau,\bar{\tau})], & \text{if } 2.5 \le r < 3.7,\ |\tau - \delta_2| = q_2; \\ \sigma_4(\zeta_0) + \sigma_3(\zeta_0) + \sigma_2(\zeta_0) \approx 0.89499, & \text{if } 3.7 \le r < 4; \\ \operatorname{Im}[W_1(\zeta_0,\tau,\bar{\tau})], & \text{if } 4 \le r < 4.5,\ |\tau - \delta_1| = q_1; \\ \sigma_4(\zeta_0) + \sigma_3(\zeta_0) + \sigma_2(\zeta_0) + \sigma_1(\zeta_0) \approx 0.91595, & \text{if } 4.5 \le r < 5; \\ \operatorname{Im}[W_0(\zeta_0,\tau,\bar{\tau})], & \text{if } 5 \le r < 6,\ |\tau| = 1; \\ 1, & \text{if } r \ge 6. \end{cases} \tag{5.1}$$

Here, the notation δ_j and q_j denote the centre and the radius of the circle C_j, $j = 1,2,3,4$ respectively. Also, $r = |f(\tau) - z_0|$.

Fig. 5.2 shows the graphs of the calculated (blue) and simulated (red) h-function for the above domain Ω_5 with basepoint $z_0 = 5.5$.

Next, we report the h-function of the septuply connected domain $\Omega_7 = \mathbb{C}\backslash(\{|z| \le 0.5\} \cup \{|z - 1.25| \le 0.25\} \cup \{|z - 2.4| \le 0.6\}) \cup \{|z - 3.6| \le 0.4\} \cup \{|z - 4.75| \le 0.25\} \cup \{|z - 5.3| \le 0.1\} \cup \{|z - 6.25| \le 0.25\}$ with basepoint $z_0 = 7$ which is strictly to the right of all discs on the boundary $\partial\Omega_7$. Fig. 5.3 shows the h-function graph of this domain Ω_7 with basepoint $z_0 = 7$. We omit the details of the calculation.

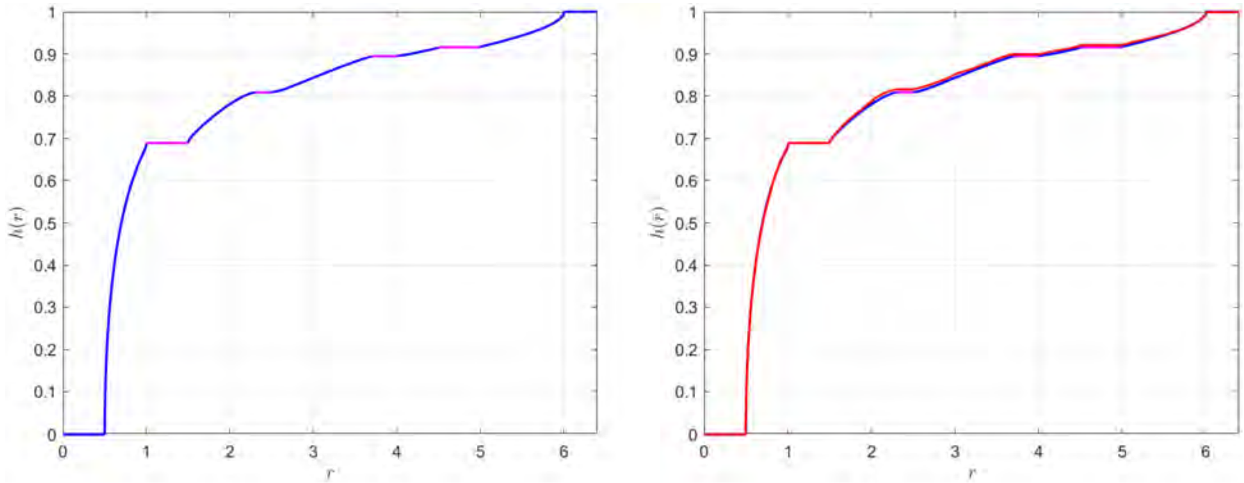

Fig. 5.2. Calculated h-function (left), and combination of calculated and simulated h-function (right) for quintuply domain $\Omega_5 = \mathbb{C}\backslash(\{|z| \leq 0.5\} \cup \{|z-1.25| \leq 0.25\} \cup \{|z-2.4| \leq 0.6\}) \cup \{|z-3.6| \leq 0.4\} \cup \{|z-4.75| \leq 0.25\}$ with basepoint $z_0 = 5.5$. The step heights are shown in magenta colour.

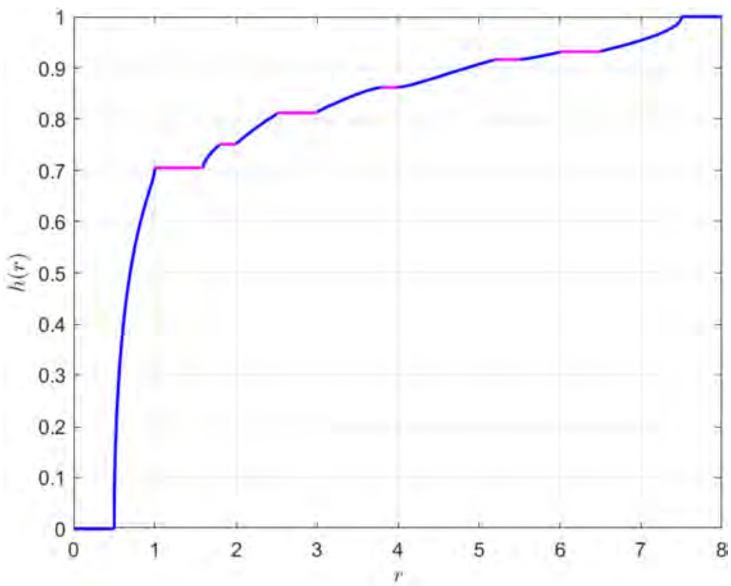

Fig. 5.3. Calculated h-function graph for septuply connected domain $\Omega_7 = \mathbb{C}\backslash(\{|z| \leq 0.5\} \cup \{|z-1.25| \leq 0.25\} \cup \{|z-2.4| \leq 0.6\}) \cup \{|z-3.6| \leq 0.4\} \cup \{|z-4.75| \leq 0.25\} \cup \{|z-5.3| \leq 0.1\} \cup \{|z-6.25| \leq 0.25\}$ with basepoint $z_0 = 7$. The step heights are shown in magenta colour.

6. Conclusion

In this paper, we have computed h-functions for some of the planar multiply connected unbounded domains whose boundary components are collinear slits of unequal size or circles of unequal size when the basepoint is located to the left or right of all boundary components. Also, we have cross-checked all the h-functions found in this paper by using numerical simulation of Brownian motion.

In the future direction of our work, we plan to extend our computation for the h-functions of domains with connectivity greater than two, to cover the case when the basepoint is fixed in between two of the boundary components. Also, it would be of interest to determine the asymptotics of h-functions for multiply connected domains.

An ambitious goal is to compute the h-functions for multiply connected non-planar domains.

Acknowledgments

The author sincerely thanks Lesley Ward and Christopher Green for their support.

References

[1] J. Aarao, M.A. Snipes, B.L. Walden, l.A. Ward, Four ways to calculate harmonic measure in a doubly connected domain, Unpublished notes.
[2] H.F. Baker, Abelian Functions: Abel's Theorem and the Allied Theory of Theta Functions, Cambridge University Press, Cambridge, 1897.
[3] D.A. Brannan, W.K. Hayman, Research problems in complex analysis, Bull. Lond. Math. Soc. 21 (1) (1989) 1–35.
[4] D. Crowdy, J. Marshall, Conformal mappings between canonical multiply connected domains, Comput. Methods Funct. Theory 6 (1) (2006) 59–76.
[5] D.G. Crowdy, J.S. Marshall, Computing the Schottky–Klein prime function on the Schottky double of planar domains, Comput. Methods Funct. Theory 7 (1) (2007) 293–308.
[6] D. Crowdy, Geometric function theory: a modern view of a classical subject, Nonlinearity 21 (10) (2008) T205–T219.
[7] D. Crowdy, Conformal slit mappings in applied mathematics, ANZIAM J. 53 (3) (2012) 171–189.
[8] D. Crowdy, Solving Problems in Multiply Connected Domains, CBMS-NSF Regional Conference Series in Applied Mathematics, vol. 97, Society for Industrial and Applied Mathematics, Philadelphia, 2020.
[9] D.G. Crowdy, E.H. Kropf, C.C. Green, M.M.S. Nasser, The Schottky–Klein prime function: a theoretical and computational tool for applications, IMA J. Appl. Math. 81 (3) (2016) 589–628.
[10] Imperial College London Applied and Computational Complex Analysis group GitHub website, https://github.com/ACCA-Imperial.
[11] C.C. Green, A. Mahenthiram, L.A. Ward, Harmonic-measure distribution functions of multiply connected domains with various geometries, in preparation.
[12] C.C. Green, A. Mahenthiram, L.A. Ward, Constructive solution of the inverse problem for harmonic-measure distribution functions that are step functions, in preparation.
[13] C. Green, Mathematical techniques for free boundary problems with multiple boundaries, PhD Thesis, Imperial College London, 2013.
[14] C.C. Green, M.A. Snipes, L.A. Ward, D.G. Crowdy, Harmonic-measure distribution functions for a class of multiply connected symmetrical slit domains, Proc. R. Soc. A, Math. Phys. Eng. Sci. 478 (2259) (2022) 20210832.
[15] D.A. Hejhal, Theta Functions, Kernel Functions and Abelian Integrals, Memoirs of the American Mathematical Society, vol. 129, 1972, iii+112 pp.
[16] J. Marshall, Function theory in multiply connected domains and applications to fluid dynamics, PhD Thesis, Imperial College London, 2005.
[17] A. Mahenthiram, Harmonic-measure distribution functions, and related functions, for simply connected and multiply connected two-dimensional regions, PhD Thesis, University of South Australia, 2022.
[18] A. Mahenthiram, Computing h-functions of some planar simply connected two-dimensional regions, Taiwan. J. Math. 27 (5) (2023) 931–952.
[19] A. Mahenthiram, Harmonic-measure distribution functions of simply connected and doubly connected polygonal domains, J. Math. Anal. Appl. 537 (1) (2024) 128308.
[20] A. Mahenthiram, New harmonic-measure distribution functions of some simply connected planar regions in the complex plane, Rev. Unión Mat. Argent. (2025), https://doi.org/10.33044/revuma.4038, in press.
[21] A. Mahenthiram, B.L. Walden, L.A. Ward, Harmonic-measure distribution functions for new planar simply connected regions, and behaviour of their derivatives, in preparation.
[22] M.A. Snipes, L.A. Ward, Harmonic measure distributions of planar domains: a survey, J. Anal. 24 (2) (2016) 293–330.
[23] T.W. Ng, C.C. Tang, J. Tsai, The squeezing function on doubly-connected domains via the Loewner differential equation, Math. Ann. 380 (3) (2021) 1741–1766.
[24] B.L. Walden, L.A. Ward, Distributions of harmonic measure for planar domains, in: I. Laine, O. Martio (Eds.), Proceedings of 16th Nevanlinna Colloquium, Joensuu, Walter de Gruyter, Berlin, 1996, pp. 289–299.